ОБЪЕДИНЕННЫЙ
ИНСТИТУТ
ЯДЕРНЫХ
ИССЛЕДОВАНИЙ

Дубна

E15-98-337

NOVEL METHOD FOR MCF STUDY IN A DENSE D/T MIXTURE, FIRST EXPERIMENTAL RESULTS

Submitted to «Hyperfine Interactions»

1998

Yu.P.Averin[1], D.V.Balin[2], V.R.Bom[3], J.N.Bradbury[4], J.D.Davies[5], A.M.Demin[1], D.L.Demin, A.E.Drebushko, V.P.Dzhelepov, C.W.E. van Eijk[3], V.V.Filchenkov, A.N.Golubkov[1], N.N.Grafov, V.G.Grebinnik, S.K.Grishechkin[1], V.G.Klevtsov[1], A.D.Konin, A.A.Kukolkin[1], S.V.Medved', A.B.Modenov[1], V.A.Nazarov[1], V.V.Perevozchikov[1], V.I.Pryanichnikov, V.Ya.Rozhkov[1], A.I.Rudenko, S.M.Sadetsky[2], G.G.Semenchuk[2], V.T.Sidorov, Yu.V.Smirenin[2], I.I.Sukhoi[1], V.V.Travkin[1], N.I.Voropaev[2], A.A.Yukhimchuk[1], V.G.Zinov, S.V.Zlatoustovskii[1]

[1] Russian Federal Nuclear Center, All-Russian Research Institute of Experimental Physics, 607200, Sarov, Russia
[2] St.Petersburg Nuclear Physics Institute, Gatchina, Russia
[3] Delft University of Technology, 2629 JB Delft, The Netherlands
[4] Los Alamos National Laboratory, Los Alamos, NM 87545, USA
[5] Rutherford Appleton Laboratory, Chilton, Didcot Oxon, OX11 0QX, UK

1 Motivation

The goal of the experiment is to measure the "effective" characteristics of the $d+t$ fusion cycle. The main parameters are the cycling rate λ_c and the sticking probability ω_s of muons to the Helium-4 nucleus (see Fig. 1).

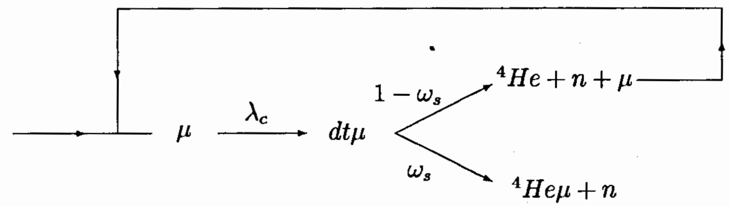

Figure 1: Simplified scheme of the $d+t$ fusion cycle

The first experimental results for this process were obtained in Dubna almost 20 years ago [1]. Then this process was widely experimentally studied by other authors, mainly at LAMPF and PSI (see, for example [2, 3, 4]). The necessity of new measurements is caused by the following considerations.

Till now there were no experimental data for a dense triple H/D/T mixture where theory predicts increased cycling rates due to epithermal effects. As to a dense D/T mixture, most previous measurements were made by the "standard" methods where only the product $\omega_s\lambda_c$ is directly measured. In the present work new methods of the analysis are employed which enable us to directly determine the values of ω_s and λ_c for a dense hydrogen isotope mixture.

2 Experimental method

The principal features of our experimental method [6, 7, 8, 9] are the following:
1. A high efficiency neutron detection system is used in close to 4π geometry.
2. For muon and electron registration we use specially designed proportional counters with very low sensitivity to neutrons from the $d+t$ reaction.
3. To eliminate the distortions in the neutron time spectra caused by possible pile up, the charge time distributions for the neutron detector signals are measured, contrary to the usually registered time distributions of the number of events.
4. Novel methods of the data analysis are used. They consist in consideration of the last neutron - electron time spectra and the neutron multiplicity distributions.

The experimental equipment have been described in [8]. The installation has been mounted on the muon beam of the JINR phasotron at the Laboratory of Nuclear Problem (LNP). The main parts of the experimental set-up are a compact cryogenic target with volume 30 ccm [10], a filling system for hydrogen isotopes of high purity [11], a wire electron counter [12] and a full absorption neutron spectrometer [13], consisting of two identical detectors (ND1 and ND2).

Pulses from the PM of the neutron spectrometer are registered by FADC's (8 bit x 2048 samples, 100 Mc/s) producing a time distribution of the detector amplitude for each single muon. To provide correct time measurements the signal of the detector for incoming muons and of the electron counter are also analyzed by FADC's. The first signal serves as a reference and the second one is used to measure the time of the electron from μ-decay. A trigger device based on Filed Programmable Gate Array IC [14] was used in this experiment.

3 Measurements

The experimental conditions for different exposures are given in Table 1.

Table 1. Experimental conditions for runs with the liquid tritium target

Exp.	Tritium concentration, %	Temperature, K	Density, (in LHD)	Molecular content, % DD	DT	TT
1	0	21.3(0.1)	1.18(0.02)	98(1)	0	0
2	18.9(2.4)	21.7(0.1)	1.19(0.03)	64.6(1.9)	31.9(1.9)	2.9(0.1)
3	64.1(2.0)	21.8(0.1)	1.23(0.03)	9.4(1.7)	51.8(1.7)	38.1(1.1)
4	57(2)	38.5(2)	0.145(0.004)	19(0.5)	47(2)	33(1)
5	35.8(1.9)	22.6(0.1)	1.19(0.03)	40.3(1.4)	47.2(1.4)	12.1(0.4)
6	88.5(2.6)	22.2(0.1)	1.24(0.03)	3.0(1.5)	15.9(1.5)	80.2(2.4)
7	33.9(1.3)	22.4(0.1)	1.20(0.02)	42.4(0.9)	46.8(0.9)	10.5(0.2)

Exposure 1 with D_2 was made to have the electron timing spectrum in "pure" condition (without $d+t$ neutrons). In addition, one exposure was made with empty target to determine the background for electron spectra. Exposure 4 with a low density gas mixture was mainly done to provide the correct charge calibration when pile-up effects are negligible. The tritium concentrations and molecular contents were obtained by chromotography immediately before and after each exposure and then corrected for the cryogenic isotope separation.

During the run the main distributions were plotted and analyzed. The timing spectra of all detected neutrons were obtained by summing all individual distributions of the ND signal amplitude in time [9]. A typical example of these "oscillogramms" is shown in Fig. 2. Note that this is the first "photograph" of a $d+t$ neutron series!

As is seen from Fig. 2 the time distribution of the ND signal amplitude for an individual muon is a entity of amplitude groups ("clusters" [9]). We will call the sum of the amplitudes within a cluster *cluster charge.*

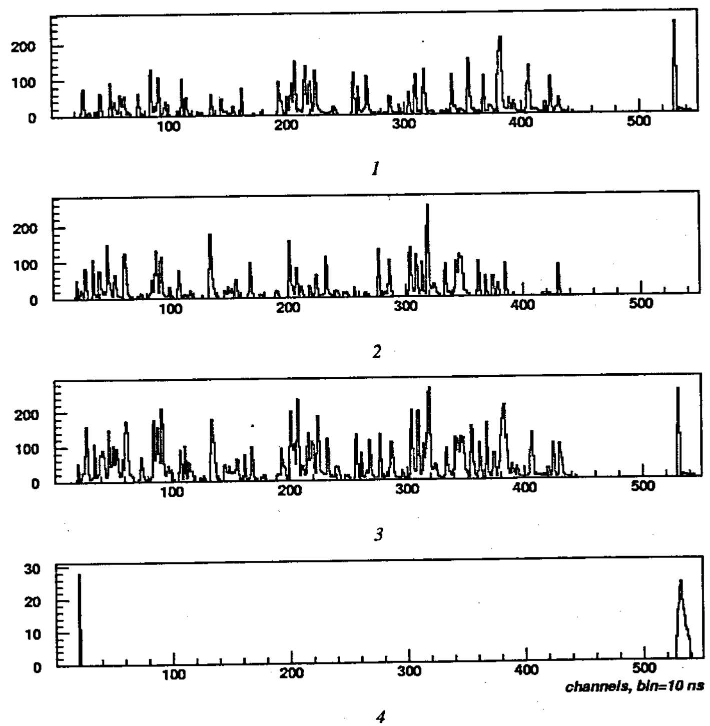

Figure 2: FADC signals for a single muon. The signals are shown for ND1 (1), ND2 (2) ND1 and ND2 together (3) and for the muon and electron detectors (4)

4 Analysis

1. Methods. In the "standard" method the time distribution of all detected neutrons is analyzed. This distribution has the well known one-exponent form

$$dN_n/dt = \epsilon_n \Lambda_c exp[-(\lambda_0 + w\Lambda_c)t] \quad (1)$$

Here $\Lambda_c = \lambda_c\phi$; ϕ is the hydrogen density, relative to the value $4.25 \cdot 10^{22}\, nuclei/cm^3$, $\lambda_0 = 0.455 \cdot 10^5\, s^{-1}$ is the free muon disappearance rate, ϵ_n is the neutron detection efficiency; w is the effective sticking probability taking also into account muon sticking in the $d+d$ and $t+t$ reactions.

The novel analysis methods used in the present work make it possible to direct measure the values of λ_c and ω_s. In [6] it was suggested to measure the distribution $N_{ne}(t)$ which is a function of the interval $t = t_e - t_n$ between the last detected neutron of the series and the μ-decay electron. This distribution has the form of a sum of two exponents with significantly different slopes

$$dN_{ne}/dt = (\lambda_0/\lambda_n)\cdot[w\cdot\Lambda_c\cdot exp(-\lambda_0\cdot t) + \epsilon_n\cdot\Lambda_c\cdot(1-w)\cdot exp(-(\lambda_0+\lambda_n)\cdot t)], \quad (2)$$

where λ_n is expressed as

$$\lambda_n = (\epsilon_n + w - \epsilon_n\cdot w)\cdot\Lambda_c \quad (3)$$

The first ("slow") exponent corresponds to the events with muon sticking and the second ("fast") one to the events without sticking. The ratio of the slow and fast amplitudes of these exponents just determine the value of w: $A_s/A_f = w/\epsilon_n(1-w)$.

The next idea [7] was to measure the neutron multiplicity (number of detected neutrons, k, per muon) distribution in some definite interval T. If one selects the events for which the muon life time is $\tau_\mu > T$ then this distribution would be a sum of two terms. One of them, the Gaussian (Poisson) with the mean $m = \epsilon_n\Lambda_c\cdot T$, corresponds to the events without sticking, and the other, depending on w and falling with k, is the distribution of events with muon sticking:

$$N(k) = N_1\cdot[f(k) + (1-w/\epsilon_n)^m\cdot g(k;m)], \quad (4)$$

where N_1 is the total number of the first detected neutrons in the interval T, $g(k;m)$ is a Gaussian and $f(k)$ is described by:

$$f(k) = y_{k-1} - y_k = y_1\cdot[1 - y_1\cdot(1-\omega)]\cdot[y_1\cdot(1-\omega)]^{k-1}, \quad (5)$$

where $y_1 = \epsilon_n\Lambda_c/\lambda_n = (1 - w/\epsilon_n - w)^{-1}$ is the relative yield of the first detected neutrons. This expression is valid for $m >> 1$. (In addition, the "right edge" effect must be taken into account in the correct analysis.)

Again, as in the previous method, there is a separation of the events with and without sticking. An important advantage of the suggested methods is that the normalization to the electron number is not required in them. Later we will call, for short, these methods as "$t_e - t_n$ method" and "multiplicity" one.

2. Charge calibration. This was made on the basis of the data obtained in an exposure with a gaseous D/T mixture of relatively low density where each cluster corresponds practically to one neutron. So the mean average charge is $q = Q/N_{cl}$, where Q is the total charge and N_{cl} is the number of clusters.

3. Fit and calculations. In the standard method the procedure is well known. From the fit of the charge-normalized time distribution of all detected neutrons with formula (1) one obtaines the total number of neutrons N_n and the exponent slope $\lambda = \lambda_0 + w\Lambda_c$. The number of electrons N_e found from an anlysis of the electron time spectrum was used for the absolute normalization. So,

$$\epsilon_n\Lambda_c = N_n/N_e; \qquad w/\epsilon_n = (\lambda - \lambda_0)/\epsilon_n\Lambda_c. \quad (6)$$

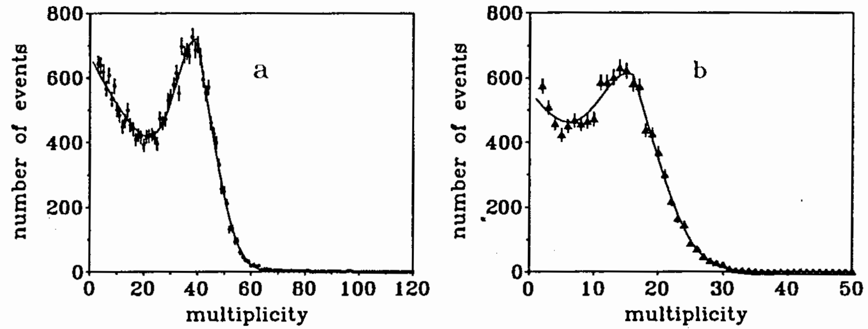

Figure 3: Neutron multiplicity distributions. Spectrum "a" corresponds to the exposure with $C_T = 35.8\,\%$ and was plotted for both ND and time interval $T = 1\,\mu s$. Variant "b"was selected for $C_T = 88.5\,\%$, both ND and $T = 2\,\mu s$. Curves are the optimum fits.

Examples of the neutron multiplicity distributions (again charge normalized) for Exp. 6-7 are given in Fig. 3. Such distributions for each exposure were fitted with formula (4). The quantities w/ϵ_n and the Gaussian (Poisson) mean $m = \epsilon_n\Lambda_c T$ were variable parameters. Other parameters were the total number of events and the dispersion of the Gaussian. The optimal fit is shown by the curve.
The $t_e - t_n$ spectra for Exp. 6-7 are shown in Fig. 4. Such distributions were analyzed with use of the expressions (2-3). The optimal values of w/ϵ_n and $\lambda_n\epsilon_n$ were obtained directly from the fit. So, for all considered methods of analysis we obtained a set of values $\epsilon_n\Lambda_c$ and w/ϵ_n. To extract the values of Λ_c and w one should know ϵ_n.

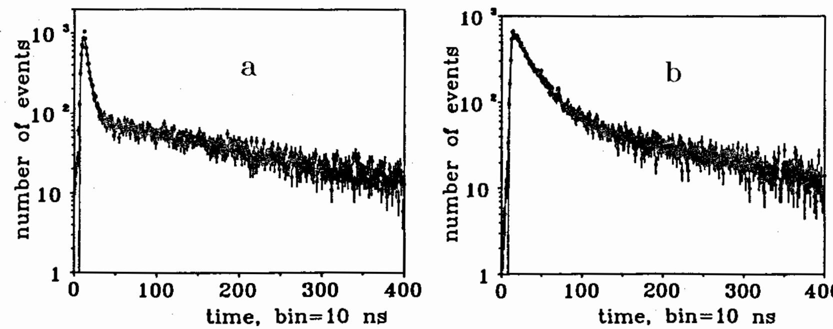

Figure 4: Electron - last neutron timing spectra. Spectrum "a" corresponds to the exposure with $C_T = 35.8\,\%$ and variant "b"was selected for $C_T = 88.5\,\%$

4. The neutron detection efficiency. The quantity ϵ_n as a function of the energy (charge) threshold was calculated by the Monte-Carlo (M-C) method. The special code **NEFF** has been created for this aim [15]. "Closed" geometry of the experiment and the use of the neutron detectors of large size gave rise to a significant effect(25% for zero threshold) of neutron rescattering from one detector to another with simultaneous registration by both of them. In Exp. 4 with a mixture of low density we could separate "single" events and "coincident"ones. For the energy threshold $E_{th} = 1.5\,MeV$ the values of the rescattering fraction are equal to 0.134 (calculations) and 0.146 (measurements). The total efficiency ("single" and "coincident") was calculated to be $\epsilon_n = 13.5\,\%$. Corrections to the efficiency for the pile-up effects were calculated with the special code **SIMFADC** [9].

5 Results

At present the analysis has not been completed. Now we are ready to present only tentative data on the cycling rate and the muon sticking probabilty ω_s. They are given in Table 2 and Fig. 5. Now we are not ready to present the values of w obtained by the $t_e - t_n$ method for the first run where a strong trigger was used.

The errors in the values presented in the table combine statistical (fit) and possible systematic uncertainties estimated from the selection and charge calibration procedures. The results are given for both ND together. The spread between the data for ND1 and ND2 is in the limit of the presented errors. One should consider separately the systematic error in the value of ϵ_n. According to our estimations, it is ±5%.

Table 2. Values of cycling rates (Λ_c) and effective muon losses (w) obtained by the three analysis methods

Method	Quantity	Tritium concentration, %					
		18.9	33.9	35.8	57	64.1	88.5
Standard	$\lambda_c\phi$, μs^{-1}	75(4)	145(7)	146(7)	4.2(2)	113(5)	28(1)
	w, %	0.79(4)	0.64(3)	0.64(3)		0.73(4)	1.48(7)
Muliplicity	$\lambda_c\phi$, μs^{-1}	73(2)	141(4)	140(4)		108(3)	27(1)
	w, %	0.83(3)	0.65(2)	0.71(3)		0.79(3)	1.42(6)
$t_e - t_n$	$\lambda_c\phi$, μs^{-1}	70(4)	137(7)	143(7)		110(5)	28(1)
	w, %		0.63(3)				1.49(7)

As is seen from the table there is a good agreement between the results obtained by three different methods. This gives us an assurance of relaibility and validity of them.

The data obtained are shown in Fig. 5 as a function of the tritium concentration. Our data for λ_c are given for the muliplicity method as the most reliable. The systematic uncertainty caused by the ϵ_n is not included. The values of the other authors were taken from [16].

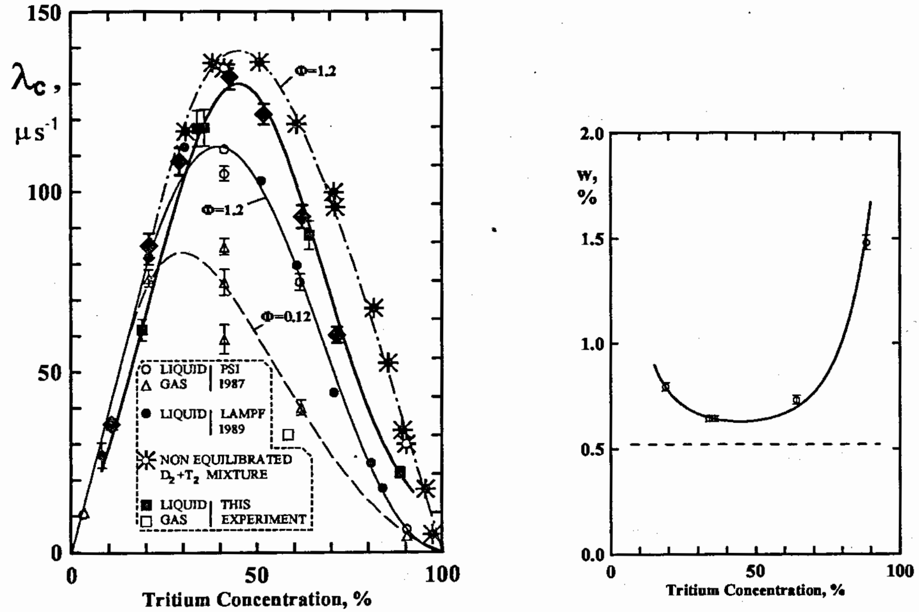

Figure 5: Normalyzed cycling rates and effective muon loss factors as functions of tritium concentration. The data for λ_C is taken from [16], our data are shown by squares and the data [17] by rhombs

The values of λ_c were analyzed using the expression

$$\frac{1}{\lambda_c} \simeq \frac{C_d q_{1S}}{C_t \lambda_{dt}} + \frac{3/4}{C_t \lambda_{1-0}} + \frac{1}{C_{D_2}\lambda^0_{dt\mu-d} + C_{DT}\lambda^0_{dt\mu-t}} \tag{7}$$

with the approximation $q_{1S} = 1/(1 + aC_t)$. The parameters of fomula (7) are very sensitive to the molecular concentrations. Therefore, these concentrations were considered variable in the limits of their uncertainities. The analysis results are $a = 2.1 \pm 0.3$ and

$$\lambda_{dt\mu-d} = (823 \pm 80 \pm 41)\,\mu s^{-1} \tag{8}$$

The last error in (8) is the uncertainty from the ϵ_n calculation. Our value of $\lambda_{dt\mu-d}$ it is noticeably higher than the value $450 - 500\,\mu s^{-1}$ found in [18]. A possible source of a disagreement might be connected with different molecular contents in the target. The final conclusion may be drawn after *direct observation* of the molecular content inside the target (Raman spectrometry) during the run.

The values of w presented in Fig. 5 were fitted with use of the expression

$$w \simeq \omega_s + \frac{\lambda_{tt\mu}\omega_{tt}\lambda_f^{tt}}{\lambda_{dt\mu}(\lambda_f^{tt} + \lambda_{tt\mu})} + \frac{2}{3}\frac{C_d q_{1S}\lambda^{3/2}_{dd\mu}C_{DD}\omega_{dd}}{\lambda_{dt} + (1 - q_{1S})\lambda_{dd\mu}} + \lambda_Z C_Z/\lambda_c \tag{9}$$

It is the same as in [4] but the term $\Lambda_Z C_Z/\Lambda_c$ is added which takes into account the muon transfer to an inpurity with $Z > 1$.

Analyzing the expression (9) we used the values (8). The quantities ω_s, $\lambda_{tt\mu}\omega_{tt}$ and $\Lambda_Z C_Z$ were variable parameters. The results are $\lambda_{tt\mu}\omega_{tt} = (0.13 \pm 0.06)\,\mu s^{-1}$ (measured value is $(0.25 \pm 0.08)\,\mu s^{-1}$) and $\Lambda_Z C_Z = (0.07 \pm 0.04)\,\mu s^{-1}$, which is in agreement with an estimation $(0.08 \pm 0.04)\,\mu s^{-1}$ based on the analysis of the electron time spectra.

The main result is

$$\omega_s = (0.533 \pm 0.040 \pm 0.025)\% \qquad (10)$$

This value is shown by the dashed line in Fig. 5. It is in satisfactory agreement with two results obtained previously for the liquid D/T mixture at PSI [4, 5] and LAMPF [3]:

$$\omega_s = (0.45 \pm 0.05)\% \, [PSI] \, [4,\ 5], \quad \omega_s = (0.43 \pm 0.05 \ \pm 0.06)\% \, [LAMPF] \, [3].$$

6 Acknowledgments

The authors thank Prof. L.I. Ponomarev for his assistance and help to this experiment. The financial support of the International Science and Technology Center (grant No 025-95) and RFBR (grant No 97-02-16882) is acknowledged with gratitude.

References

[1] V.M. Bystritsky et al, Phys. Lett. 94B (1980) 476, JETP 53(1981)877.

[2] S.E. Jones et al, Phys. Rev. Lett. 56(1986)588;
A.J. Caffrey et al, Muon Cat. Fusion 1(1987)53.

[3] S.E. Jones, Hyp. Int., 82(1993)303.

[4] W.H. Breunlich et al, Phys. Rev. Lett. 58(1987)329;
Muon Cat. Fusion 1(1987)67.

[5] C. Petitjean et al., Hyp. Int., 82(1993)273.

[6] V.G. Zinov, Muon Cat. Fusion 7(1992)419.

[7] V.V. Filchenkov, Muon Cat. Fusion 7(1992)409.

[8] D.L. Demin et al, Hyp. Int. 101/102(1996)591.

[9] V.V. Filchenkov, A.E. Drebushko, A.I. Rudenko, Nucl. Instr. and Meth. A 395(1997)237.

[10] D.L. Demin et al., Proc. of the Int. Workshop EXAT−98, 19 – 24 July 1998, Ascona, Switzerland.

[11] A.A. Yukchimchuk et al., Proc. of the Int. Workshop EXAT−98, 19 – 24 July 1998, Ascona, Switzerland.

[12] A.D. Konin, Preprint JINR P13-82-634, Dubna, 1982.

[13] V.P. Dzhelepov et al., Nucl. Instr. and Meth., A 269(1988)634.

[14] A.I. Rudenko, V.T. Sidorov, V.G. Zinov. Perprint JINR, P13-96-439, 1996.

[15] V.R. Bom and V.V. Filchenkov, Proc. of the Int. Workshop EXAT−98, 19 – 24 July 1998, Ascona, Switzerland.

[16] C. Petitjean, Nuclear Physics A543 (1992) 79c.

[17] K. Nagamine et al., Proc. of the Int. Workshop EXAT−98, 19 – 24 July 1998, Ascona, Switzerland.

[18] P. Ackerbauer et al., Proc. of the Int. Workshop on Low Energy Muon Science - LEMS'93, Los-Alamos, p. 285; Los Alamos Report LA-12698-C.

Received by Publishing Department
on December 8, 1998.